
ConvMAE: Masked Convolution Meets Masked Autoencoders

Peng Gao¹ Teli Ma¹ Hongsheng Li² Jifeng Dai³ Yu Qiao¹
¹ Shanghai AI Laboratory ² MMLab, CUHK
³ SenseTime Research

Abstract

Vision Transformers (ViT) become widely-adopted architectures for various vision tasks. Masked auto-encoding [2, 1, 26, 57] for feature pretraining and multi-scale hybrid convolution-transformer architectures [10, 20, 51, 32, 59] can further unleash the potentials of ViT, leading to state-of-the-art performances on image classification, detection and semantic segmentation. In this paper, our ConvMAE framework demonstrates that multi-scale hybrid convolution-transformer can learn more discriminative representations via the mask auto-encoding scheme. However, directly using the original masking strategy leads to the heavy computational cost and pretraining-finetuning discrepancy. To tackle the issue, we adopt the masked convolution to prevent information leakage in the convolution blocks. A simple block-wise masking strategy is proposed to ensure computational efficiency. We also propose to more directly supervise the multi-scale features of the encoder to boost multi-scale features. Based on our pretrained ConvMAE models, ConvMAE-Base improves ImageNet-1K finetuning accuracy by 1.4% compared with MAE-Base. On object detection, ConvMAE-Base finetuned for only 25 epochs surpasses MAE-Base finetuned for 100 epochs by 2.9% AP^{box} and 2.2% AP^{mask} respectively. Code and pretrained models are available at <https://github.com/Alpha-VL/ConvMAE>.

1 Introduction

Self-supervised learning frameworks, such as DINO [5], MOCO-V3 [8], MAE [26], unleash the potential of Vision Transformers (ViT) and achieve strong performance on various vision downstream tasks [31, 28, 60]. Mask Autoencoders (MAE) [26] is the recent representative self-supervised method for training ViT. Motivated by BERT [13] in natural language processing, feature pretraining is conducted via a novel asymmetric encoder and decoder architecture, in which masked tokens of the encoder are reconstructed by the decoder. Discriminative and scalable vision representations can be learned from ImageNet-1K [12] without relying on large-scale datasets, such as ImageNet-22K or JFT300M.

Along with the successes of self-supervised learning, local inductive bias [51, 20, 32, 10, 17, 59] and hierarchical representations [41, 56] are explored for boosting the performance of ViT. The combination of local convolution and global transformer operations have shown significantly improvements on image classification [31], object detection [28], and semantic segmentation [60]. In contrast to MAE [26], well-performing multi-scale backbones built upon local and global operations are mainly trained with supervised learning approaches. A natural question is whether multi-scale backbone with local and global operations, which show promising performance on supervised learning can be enhanced by the masked auto-encoding paradigm [26, 13, 2, 66].

In this paper, a simple and effective self-supervised learning framework, dubbed as ConvMAE, is proposed to train scalable representations by introducing hybrid convolution-transformer architectures and masked convolution into the masked auto-encoders. Although the modifications to the original MAE are minimal, ConvMAE shows great success on pretraining visual representations for boosting

the performances of various tasks. Compared with MAE-Base [26], ConvMAE-Base improves the ImageNet-1K finetuning accuracy to 85.0% (+1.4%), COCO detection AP^{box} to 53.2% (+2.9%) with Mask-RCNN, ADE20k mIoU to 51.7% (+3.6%) with UperNet, respectively.

Different from MAE [26], the encoder of ConvMAE progressively abstracts the input image into multi-scale token embedding of 1/4, 1/8, 1/16 input resolutions at stages 1, 2, 3, respectively, while the decoder reconstruct the pixels corresponding to masked tokens by utilizing multi-scale token embeddings. For low-level high-resolution token embedding at stages 1 and 2, convolutions blocks are adopted for encoding local information. For high-level low-resolution token embedding at stage 3, transformer blocks are used for aggregating global context. The encoder therefore has local/global FOV at different stages and generates discriminative multi-scale features. Note that the ConvMAE encoder is highly motivated by the strong hybrid convolution and transformer backbones, including Co-AtNet [10], Early Convolution [59], Container [20] and Uniformer [32]. However, such hybrid convolution-transformer networks were either not explored for masked auto-encoding [20, 32, 18] or show very similar performance to MAE [54, 61]. Instead of designing novel architectures, we focus on making basic hybrid convolution-transformer architectures work for mask auto-encoding and conduct extensive experiments to demonstrate its effectiveness on various downstream tasks.

The efficient and effective training of ConvMAE is enabled by a block-wise masking strategy with masked convolution [62, 23, 30, 49, 22, 39]. The masking strategy adopted in current mask-autoencoding frameworks, such as BEiT [2], MAE [26], SimMIM [61], cannot be naively used for ConvMAE as all tokens need to be kept in the later transformer stages. It would have unaffordable computation cost for pretraining large and huge models, losing MAE’s efficiency advantage of omitting masked tokens in the transformer encoder. In addition, directly pretraining with the convolution-transformer encoder causes pretraing-finetuning discrepancy as only visible tokens are processed during finetuning stages. To tackle the issues, ConvMAE adopts a block-wise masking strategy to first obtain a mask for the transformer stage-3 of 1/16 input resolution and then progressively upsamples the mask to larger resolutions of 1/8 and 1/4 for convolutional stages 2 and 1. In this way, stage-3 tokens can be completely separated into masked tokens and visible tokens and inherit the computation efficiency of MAE. To prevent information leakage, the convolution blocks at stages 1 and 2 are equipped with masked convolutions, which avoid mixing up features of masked and visible regions in stage-3 to ensue the training effectiveness. Masked convolution has been well explored in sparse feature extraction [23, 49, 22, 62] and image inpainting [39]. It can be naturally integrated into the hybrid convolution-transformer architecture to enable masked auto-encoding.

Our ConvMAE can naturally provide multi-scale features for object detection and semantic segmentation, which are required by modern detection [28] and segmentation frameworks [60]. Multi-scale features from the pretrained ConvMAE can significantly improve the performances of object detection and semantic segmentation compared MAE. ConvMAE can even surpass the fully-supervised pretraining of Swin and MViT [41, 34], with masked-based autoencoding.

In summary, our contributions can be summarized below: (1) We present the strong and efficient self-supervised framework ConvMAE, which is easy to implement but show outstanding performances on different tasks. (2) The proposed ConvMAE naturally generates hierarchical representations and exhibit promising performances on object detection and segmentation. (3) ConvMAE-Base improves the ImageNet finetuning accuracy by 1.4% compared with MAE-Base. On COCO 2017 with Mask-RCNN, ConvMAE-Base achieves 53.2% AP^{box} and 47.1% AP^{mask} with a 25-epoch training schedule while MAE-Base attains 50.3% AP^{box} and 44.9% AP^{mask} with 100 training epochs. On ADE20K with UperNet, ConvMAE-Base surpasses MAE-Base by 3.6 mIoU (48.1% vs. 51.7%).

2 Related Work

Vision Transformer. The significant progress in Natural Language Understanding(NLP) [13, 46, 3] and Multimodality Learning [52, 19, 45] during recent years is mainly promoted by Transformer Architecture [55]. Transformer Architecture [55] not only provide a high-capacity neural modules using key-query attention but also reveal a promising future for unifying all tasks and all data modalities. Vision Transformer(ViT) [16] and DETR [4] demonstrated the powerful ability of pure transformer architecture in fundamental vision tasks, achieve excellent performance compared with complex vision pipelines [50, 48, 37]. Different from the traditional well explored locality inductive bias and multi-scale representations in vision [31, 29], ViT/DETR tackle vision tasks using global,

single-scale and prior-free attention modules which result into high accuracy at the costs of slow convergence. To increase the convergence speed and improve accuracy, well-explored locality inductive bias have been reintroduced into vision transformer. In object detection, Deformable DETR [67], SMCA-DETR [21], SAM-DETR [64], DAB-DETR [40] significantly accelerate the convergence speed of DETR and improve object detection mAP with better designed locality inductive bias. Such successes have also been observed in vision backbone design [25, 63, 53, 17, 58, 24]. PVT [56] introduced multi-scale representation into ViT and achieved improved downstream transfer ability on object detection and semantic segmentation. SWIN [41] proposed a simple shift-local window mechanism for efficient intra- and inter- window communication using key-query attention. BoT [51], Early-Conv [59], Co-AtNet [10], Container [20], Uniformer [32] observe hybrid architecture of convolution and transformer design can achieve state-of-the-art performance of a wide range of tasks such as image classification, image detection, semantic segmentation, pose estimation and video understanding. Our ConvMAE is highly motivated by the hybrid architecture design [20, 32] in vision backbones. Instead of designing new architectures, ConvMAE aim to unleash the powerful representation induced by hybrid architectures through MAE-style pretraining with several insightful modifications.

Self-supervised Representation Learning. Contrastive learning and Masked Auto-encoding are two popular branches among self-supervised presentation learning. Contrastive learning aim to learn invariances by comparing augmented views of un-labeled images. SimCLR [6] exhibits simple contrastive learning can learn strong representation. MOCO [27] add a slow momentum encoder to increase the negative samples in contrastive learning. DINO [5] and MOCO-V3 [8] perform extensive studies of how to train ViT using contrastive learning. Recently, another branch of self-supervised learning, namely Mask-Autoencoding, motivated by BERT [13] raised to be a promising methodology. Without relying on building strong image augmentation employed in Contrastive Learning, Mask-Autoencoding can learn strong representation through masked patch reconstruction on randomly cropped images. BEiT [2] firstly introduced Mask-Autoencoding into Vision Community. To build a strong and scalable image learner, MAE [26] introduced an asymmetric encoder and decoder architecture where masked tokens is skipped in computation-heavy encoder and only pass all tokens through a light-weight decoder. iBoT [66] and Data2Vec [1] borrow momentum encoder and contrastive learning for improving Mask-Autoencoding. PeCo [15] introduced a perceptual tokenizer for improved representation learning. MaskFeat [57] perform ablation studies on the reconstruction target and spot masked unsupervised feature from DINO and masked HOG features are good signals for representation learning beyond masked RGB pixels and codebooks. Three Things [54] and MIMDet [18] explored the benefit of appending a convolutional stem on BEiT and MAE. Different from previous improvements of Mask-autoencoding, ConvMAE introduce hierarchical representations and multi-scale convolution-transformer architectures into MAE. We believe the useful experiences gained in PeCo [15], MaskFeat [57], iBoT [66] and Data2Vec [1] can benefit our ConvMAE.

MAE for Detection. Self-supervised pretrained backbone have shown promising results on variants of vision benchmarks among which object detection [28] is the most important and challenging vision tasks. Several works have shown promising results on adopting MAE for object detection. Benchmarking ViT [35] extracts the features from different layers of pretrained MAE encoder and generates a multi-scale feature map with dimension of $\frac{H}{4} \times \frac{W}{4}$, $\frac{H}{8} \times \frac{W}{8}$, $\frac{H}{16} \times \frac{W}{16}$ and $\frac{H}{32} \times \frac{W}{32}$ using feature adaptor. ViTDet [33] proposed a simple feature pyramid by generating multi-scale features from last layers instead of different layers proposed in Benchmarking ViT. ViTDet also removes the lateral connections inside Feature Pyramid Network(FPN) [36]. The pipeline of modern object detection [36] can be significantly simplified in ViTDet [33]. Both Benchmarking ViT and ViTDet replace original global transformer blocks with interleaving local and global transformer blocks and observe significantly decrease of GPU memory utilization and computation cost with marginal decreased object detection performance. MIMDet [18] adds a randomly initialized convolution stem to replace the large stride non-overlapping patch embedding layer employed in pretrained MAE. As convolution layer is randomly initialized, MIMDet can not achieve optimal object detection performance. Besides, MIMDet takes advantage of both MAE encoder and decoder for high-quality object detection while other approaches only adopts MAE encoder. Motivated by Benchmarking ViT [35], ViTDet [33] and MIMDet [18], we design a simple and effective way for adopting the multi-scale feature returned by ConvViT for object detection [28] and semantic segmentation [60].

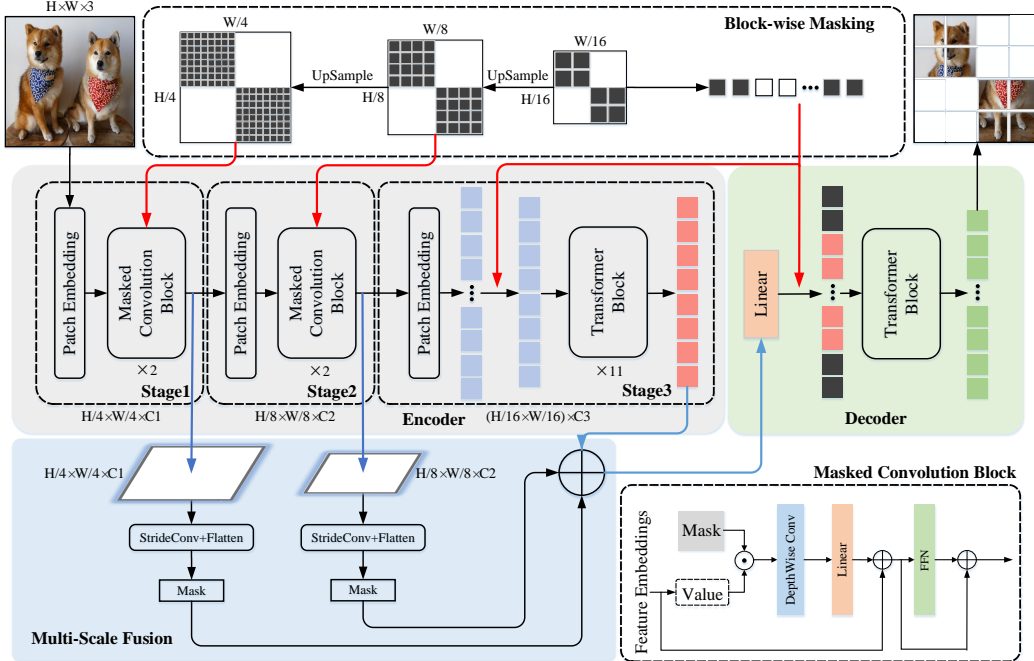


Figure 1: The pipeline of our proposed ConvMAE which consists of a hybrid convolution-transformer encoder, block-wise masking strategy with masked convolution and multi-scale decoder.

3 Approach

3.1 A Brief Revisit of MAE

Masked Autoencoders (MAE) [26] is a self-supervised method for pretraining ViT by reconstructing masked RGB patches from visible patches. Although MAE has a simple design, it has been proven to be a strong and scalable pretraining framework for learning visual presentations. MAE consists of transformer-based encoder and decoder, where only visible patches are fed into the encoder and learnable mask tokens are processed by the decoder for image reconstruction to learn visual representations. As the encoder only needs to process a small portion of visible tokens, it alleviates the scalability problem to pretrain large vision models.

3.2 ConvMAE

ConvMAE is a simple and effective derivative of the popular MAE [26] with minimal but effective modifications on the encoder design and the masking strategy. The goal of ConvMAE is to learn discriminative multi-scale visual representations and to prevent pretraining-finetuning discrepancy when applies MAE [26] on convolution-transformer networks.

Directly applying the original masking strategy on the feature maps of the convolution-transformer encoder would make transformer layers keeping all tokens during the pretraining, jeopardizing the training efficiency. We introduce a hierarchical masking strategy coupled with masked convolution for the convolution stages to ensure only a small number of visible tokens are input into the transformer layers. The overall pipeline of ConvMAE is shown in Figure 1.

The Hybrid Convolution-transformer Encoder. There are previous strong hybrid convolution-transformer architectures, such as Co-AtNet [10], Container [20], BoTNet [51], Uniformer [32] and Early Conv [59]. Without using such complicated architectures, we show that a simple design of multi-scale convolution-transformer encoder can already learn powerful representations for various downstream tasks. As shown in Figure 1, our encoder consists of 3 stages with output spatial resolutions of $\frac{H}{4} \times \frac{W}{4}$, $\frac{H}{8} \times \frac{W}{8}$, $\frac{H}{16} \times \frac{W}{16}$, respectively, where $H \times W$ is the input image resolution. The first two convolutional stages use convolution blocks to transform the inputs to token embeddings $E_1 \in \mathbb{R}^{\frac{H}{4} \times \frac{W}{4} \times C_1}$ and $E_2 \in \mathbb{R}^{\frac{H}{8} \times \frac{W}{8} \times C_2}$. Our convolution blocks follow the design principle of the transformer block by only replacing the self-attention operation with the 5×5 depthwise

convolution The third transformer stage uses commonly used self-attention blocks to obtain token embeddings $E_3 \in \mathbb{R}^{\frac{H}{16} \times \frac{W}{16} \times C_3}$. Between every stage, stride-2 convolutions are used to downsample the tokens to half of its previous spatial resolution. The local convolutions in stages 1 and 2 have relatively small field-of-view, the transformer blocks in stage 3 aggregate and fuse features from the coarse-grained features and extend the field of view to the whole image. Different from other ViTs, such as CPT [9], Container [20], Uniformer [32], CMT [24], Swin [41], which replace absolute position embedding [41] with relative position embedding or zero-padded convolution at the inputs of the first stage [9, 20, 32, 24], we find that adding absolute position embeddings to the inputs of the transformer stage-3 leads to the optimal performance. The class token is also removed from our encoder which shows limited influence.

Block-wise Masking with Masked Convolutions. Mask auto-encoders, such as MAE [26] and BEiT [2], adopt a random mask on the input tokens. However, the same strategy cannot be directly applied to our ConvMAE encoder. Uniformly masking stage-1 input tokens from the $\frac{H}{4} \times \frac{W}{4}$ feature maps would cause all tokens of stage-3 to have partially visible information and requires keeping all stage-3 tokens. Therefore, we propose to first generate the random mask to mask out $p\%$ (e.g., 75%) of stage-3 input tokens and upsample the mask by 2 times and 4 times to obtain the corresponding block-wise masks for masking stage-2 and stage-1 inputs, respectively. The corresponding masked tokens in the three stages are dropped in the encoding process and are reconstructed by the decoder for feature learning. In this way, ConvMAE only needs to keep as few as 25% tokens in the time-consuming transformer blocks for training and the efficiency of ConvMAE is not compromised.

However, the 5×5 depthwise convolutions in the first two stages naturally lead to receptive fields larger than the masked patches and cause information leakage when reconstructing masked tokens. To avoid such information leakage and ensure the quality of pretraining, we adopt masked convolution [23, 49] in the first two stages, so that the masked regions would never be involved in the encoding process. The use of masked convolution is crucial to the superior performance of ConvMAE and the pretraining-testing discrepancy is prevented by removing partially masked tokens from stage.

The Multi-scale Decoder and Loss. The decoder of the original MAE [26] takes as input both visible tokens E_d from the encoder and the mask tokens [Mask], and transform them in stacked transformer blocks for image reconstruction. Our ConvMAE encoder obtains multi-scale features E_1, E_2, E_3 , captures both fine- and coarse-grained image information. To better supervise the pretraining of such multi-grained representations, we downsample E_1 and E_2 to the same size of E_3 with stride-4 and stride-2 convolutions and fuse multi-grained tokens via a linear layer to obtain visible tokens E_d for inputting into the decoder,

$$E_d = \text{Linear}(\text{StrideConv}(E_1, 4) + \text{StrideConv}(E_2, 2) + E_3), \quad (1)$$

where $\text{StrideConv}(\cdot, k)$ represents stride- k convolution. The multi-scale decoder is illustrated in the bottom-left part of Figure 1. The same losses from the original MAE are used for reconstructing masked image patches and only the reconstruction of masked patches are considered in the objective function:

$$\mathcal{L} = \frac{1}{T_M} \sum_{t \in T_M} |I(t) - \hat{I}(t)|^2, \quad (2)$$

where T_M is the set of masked tokens and t is the token index. The reconstruction target I has normalized pixel values of the input images while \hat{I} are the reconstructed image.

3.3 ConvMAE for Object Detection and Semantic Segmentation

After pretraining, the proposed ConvMAE can naturally generate multi-scale feature maps, which can be processed by existing object detection and semantic segmentation heads to implement detection and segmentation.

As shown in Figure 2, to finetune ConvMAE for object detection, an E_4 feature map of $1/32$ input resolution is first obtained by 2×2 max pooling E_3 . However, as the ConvMAE stage-3 has 11 global self-attention layers (in our ConvMAE-base model) with excessive computational cost, we follow Benchmarking ViT [35] to replace all but 1st, 4th, 7th, 11th global self-attention layers in stage-3 to shifted-window local self-attention layers [41] with alternatively shifted 7×7 windows. The modified local self-attention layers are still initialized by the pretrained global self-attention layers. A global relative position bias [2, 41, 26, 35] is shared between global transformer blocks. Similarly, a local relative position bias [2, 41, 26, 35] is shared by local transformer blocks. In this way, the

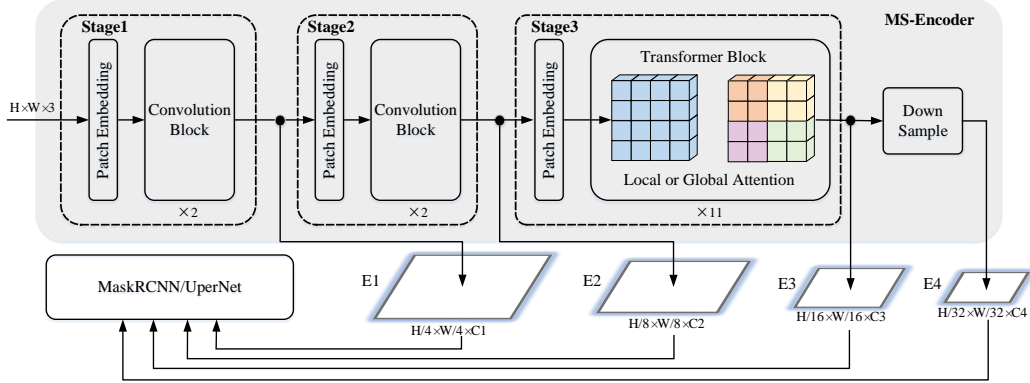


Figure 2: Overview of finetuning ConvMAE for object detection and semantic segmentation. The intermediate features of different stages serve as multi-scale inputs for an FPN [36] module.

heavy computational and GPU memory costs of the stage-3 are much mitigated. The multi-scale features E_1, E_2, E_3, E_4 are then fed into the MaskRCNN [28] head for object detection. To finetune ConvMAE for semantic segmentation, its stage-3 architecture is kept as the images in segmentation datasets have relatively smaller resolutions. The multi-scale features are input into UperNet [60] for semantic segmentation. Superior detection and segmentation performance can be achieved with the pretrained ConvMAE encoder.

4 Experiments

To validate our proposed ConvMAE, we conduct experiments of image classification on ImageNet-1K [12] dataset. The pretrained ConvMAE is also extensively tested on object detection and semantic segmentation. By default, we report performance of our the ConvMAE-base model, which has similar parameters and FLOPs as the MAE-base.

4.1 ImageNet-1K Pretraining and Finetuning

Experimental Setup. ImageNet-1K [12] consists of 1.3M images of 1k categories for image classification and is split to the training and validation sets. We pretrain our ConvMAE on ImageNet-1K training set. By default, we fix the mask ratio to 25% following the original MAE [26]. The decoder is designed to have 8 transformer layers with 512 feature dimensions and 12 attention heads. We adopt a 1600-epoch cosine learning rate schedule with the first 40 epochs for warming up. The AdamW optimizer is utilized with a base learning rate of 1.5×10^{-4} , a weight decay of 0.05 and a batch size of 1024. Random cropping is employed as data augmentation during pretraining. After pretraining, the ConvMAE encoder is used for supervised finetuning on ImageNet-1K training set for 100 epochs using the cosine learning rate schedule. We follow the default finetuning parameters of the original MAE [26] except for the layer-wise learning-rate decay parameters (0.65, 0.75, 0.85). For finetuning, we report the classification accuracy on the ImageNet validation set of the finetuned and pretrained (linear probe) ConvMAE encoders.

Results on ImageNet-1K Finetuning. We report the accuracy of ConvMAE on Table 1 and conduct

Methods	Backbone	Params. (M)	Supervision	Encoder	P-Epochs	FT (%)	LIN (%)
BEiT [2]	ViT-B	88	DALLE	100%	300	83.0	37.6
MAE [26]	ViT-B	88	RGB	25%	1600	83.6	67.8
SimMIM [61]	Swin-B	88	RGB	100%	800	84.0	56.7
MaskFeat [57]	ViT-B	88	HOG	100%	300	83.6	N/A
data2vec [1]	ViT-B	88	Momentum	100%	800	84.2	N/A
ConvMAE	ConViT-B	88	RGB	25%	1600	84.6	69.4

Table 1: Comparison with state-of-the-art mask auto-encoding schemes with similar model size. FT and LIN denotes ImageNet-1K finetuning and linear probe accuracy respectively.

comparisons with state-of-the-art mask autoencoding methods. BEiT [2] pretrains ViT-B through the

Methods	Pretraining	P-Epochs	F-Epochs	AP^{box}	AP^{mask}	Params (M)	FLOPs (T)
Benchmarking [35]	IN1K w/o labels	1600	100	50.3	44.9	118	0.9
ViTDet [33]	IN1K w/o labels	1600	100	51.2	45.5	111	0.8
MIMDET [18]	IN1K w/o labels	1600	36	51.5	46.0	127	1.1
Swin+ [41]	IN1K w/ labels	300	36	49.2	43.5	107	0.7
MViTv2 [34]	IN1K w/ labels	300	36	51.0	45.7	71	0.6
ConvMAE	IN1K w/o labels	1600	25	52.5	46.5	104	0.9

Table 2: Performances of self-supervisedly and supervisedly pretrained backbones on object detection with Mask-RCNN [28].

prediction of visual tokens tokenized by the DALL-E encoder. With 300-epoch pretraining, BEiT can reach a finetuning accuracy of 83.0% and a linear-probe accuracy of 37.6%. Compared with BEiT, ConvMAE processes only 25% visible tokens in the encoder and has a lightweight decoder for reconstruction. ConvMAE can surpass its finetuning accuracy and linear-probe accuracy by large margins (+1.9%/+31.8%). Compared with the original MAE pretrained for 1,600 epochs, our ConvMAE surpasses its finetuning accuracy by 1.3% with same number of pretraining epochs. SimMIM [61] adopts a Swin-B [41] to generate hierarchical representations. ConvMAE achieves improvement over its finetuning accuracy (+0.9%). MaskFeat [57] uses HOG [11] features as prediction targets. Data2vec [1] incorporates a momentum encoder [27] to generate predictions in an online manner. Both MaskFeat and Data2vec have higher computational costs than our ConvMAE. They can be considered as complementary directions for improving the mask auto-encoding scheme.

4.2 Object Detection

Experimental Setup. COCO dataset [38] has been widely adopted for benchmarking object detection frameworks. Mask-RCNN [28] is one of the most popular frameworks for object detection. We employ the encoder of pretrained ConvMAE as the backbone for Mask-RCNN. We finetune Mask-RCNN on COCO train2017 split and report AP^{box} and AP^{mask} on val2017 split. We follow most setups of Benchmarking ViT [35]. We report the model performance on object detection under a 25 epochs cosine schedule with a base learning rate of 8.0×10^{-5} , a weight decay of 0.1. However, limited by our GPU memory, we reduce the default batch size 64 of Benchmarking ViT [35] to 32.

Results on COCO 2017. We compare the performances of state-of-the-art visual backbones in Table 2. Benchmarking ViT [35] extensively explores using plain ViT with Mask-RCNN. Compared with Benchmarking ViT [35] finetuned for 100 epochs on COCO, ConvMAE can significantly improve AP^{box} and AP^{mask} by 2.2% and 1.6% with 25 finetuning epochs. ViTDet [33] improves Benchmarking ViT [35] by introducing a simple feature pyramid module. MIMDet [18] adds a randomly initialized convolution stem and randomly drops input tokens to increase the training efficiency of Mask-RCNN [28]. Note that MIMDet [18] introduces extra parameters due to the incorporation of MAE decoder. Compared with improved version of Benchmarking ViT [35], such as ViTDet [33] and MIMDet [18], ConvMAE achieves surpass them by 1.3% and 1.0% with a shorter finetuning schedule (25 epochs vs 100/36 epochs), fewer parameters (104M vs 111M/127M) and similar FLOPs (0.9T). This validates the effectiveness of our proposed ConvMAE framework. Swin [41] and MViTv2 [34] are state-of-the-art hierarchical visual backbones. Although adopting a simpler multi-stage architecture, ConvMAE outperforms Swin and MViTv2 by 3.3%/3% and 1.5%/0.7% in terms of $AP^{\text{box}}/AP^{\text{mask}}$. Note that Swin [41] and MViT [34] v2 are pretrained for 300 epochs with 100% tokens in a supervised manner while ConvMAE is only pretrained using masked autoencoder with 25% visible tokens, which is efficient for object detection.

4.3 Semantic Segmentation

Experimental Setup. ADE20K [65] is a widely-used semantic segmentation dataset which contains 25,562 images of 150 fine-grained categories. The dataset is split into training, validation, and testing sets. We leverage the UperNet [60], a hierarchical segmentation network head to compare ConvMAE with other backbones. Our ConvMAE with UperNet [60] is finetuned on ADE20K training set and tested on validation split. In the training phase, the backbone is initialized with the weights pretrained for 1600 epochs on ImageNet-1K and other modules are initialized with Xavier initialization. We adopt a 16k-iteration polynomial learning rate schedule with the first 1500 iterations for warming up. The AdamW [43] optimizer is adopted with an initial learning rate of 10^{-4} , a weight decay of 0.05

Models	Pretrain Data	P-Epochs	mIoU	Params (M)	FLOPs (T)
DeiT-B [53]	IN1K w/ labels	300	45.6	163	0.6
Swin-B [41]	IN1K w/ labels	300	48.1	121	0.3
MoCo V3 [27]	IN1K	300	47.3	163	0.6
DINO [5]	IN1K	400	47.2	163	0.6
BEiT [2]	IN1K+DALLE	1600	47.1	163	0.6
PeCo [15]	IN1K	300	46.7	163	0.6
CAE [7]	IN1K+DALLE	800	48.8	163	0.6
MAE [26]	IN1K	1600	48.1	163	0.6
ConvMAE	IN1K	1600	50.7	153	0.6

Table 3: Comparison with self-supervisedly and supervisedly pretrained backbones on ADE20k semantic segmentation with UperNet.

Pretrain Epochs	ImageNet		COCO		ADE20K
	FT	LIN	AP^{box}	AP^{mask}	mIoU
200	84.1	62.5	50.2	44.8	48.1
400	84.4	66.9	51.4	45.7	49.5
800	84.6	68.4	52.0	46.3	50.2
1600	84.6	69.4	52.5	46.5	50.7

Table 4: The influence of increasing pretraining epochs on image classification, object detection and semantic segmentation.

and a batch size of 16. We follow the default finetuning configurations of MAE on ADE20K except for the feature dimensions for the decoder head and the layer-wise learning rate decay is set as 0.75.

Results on ADE-20K. We report the Mean Intersection over Union (mIoU) performance of ConvMAE and other state-of-the-art backbones in Table 3. With the 300-epoch pretraining, MoCo V3 [8] can reach 47.2 mIoU when finetuned on semantic segmentation. BEiT [2], PeCo [15] and CAE [7] utilize discrete VAE as visual tokenizer to create the targets. Both BEiT and CAE adopt the DALLE [47] codebook trained on 250M images, while PeCo trains a codebook only on ImageNet-1K. Compared with these methods, our 1600-epoch pretrained MAE achieves much higher performance (50.7%). Compared with MAE pretrained 1600 epochs, our ConvMAE outperforms it by 2.6% mIoU, demonstrating the hierarchical representations of ConvMAE largely diminishes the transfer gap between pretrained backbones and downstream networks.

4.4 Ablation Study of ConvMAE

We conduct extensive ablation studies on ConvMAE to analyze different components of ConvMAE (see Table 5 and 6). To better understand ConvMAE, we also visualize the reconstructed patches, attention patterns and correlation between layers.

Pretraining epochs. For MAE, longer pretraining epochs can significantly improve the learned representations learned. We pretrain ConvMAE-Base with 200, 400, 800 and 1600 epochs to test the influences on ConvMAE. We report the ImageNet-1K finetuning (FT) and linear probe (LIN) accuracies, AP^{box} and AP^{mask} of COCO, mIoU of ADE20K on Table 4. We observe improved performances on most downstream tasks with longer pretraining epochs.

Input token random masking. As shown in Table 5, we replace the proposed block-wise mask strategy with MAE’s input token random masking. Compared with our ConvMAE-base, the ImageNet-1K finetuning accuracy drops from 84.6% to 84.2% which validates that the proposed simple block-wise masking strategy can alleviate pretraining-finetuning discrepancy. Input-token random masking results in all tokens in stage-3 being processed by computationally intensive transformer blocks and causes FLOPs to increase by $1.7\times$.

Influence of masked convolution. Masked Convolution can prevent information leakage due to the overlapping window in convolution. Removing masked convolution decreases the ImageNet-1K finetuning accuracy from 84.6% to 81.5% , which demonstrates that information leakage in convolution stages hinders feature learning in mask autoencoding.

P-Epochs	Masked Conv	Block Masking	5×5 Conv	7×7 Conv	9×9 Conv	FT (%)	FLOPs
800	✓	✓	✓	✗	✗	84.6	1×
	✓	✗	✓	✗	✗	84.2	1.7×
	✗	✓	✓	✗	✗	81.5	1×
	✓	✓	✓	✗	✗	84.5	0.997×
	✓	✓	✗	✓	✗	84.4	1.003×
	✓	✓	✗	✗	✓	84.6	1.007×

Table 5: Ablation study on the influence of the masked conv, block masking, kernel size in stages 1 and 2 of ConvMAE on ImageNet-1K finetuning accuracy.

P-Epochs	Method	FT (%)	LIN (%)	AP^{box}	AP^{mask}	mIoU
200	ConvMAE-Base	84.1	N/A	50.2	44.8	48.1
	w/ multi-scale decoder	84.4	N/A	50.8	45.4	48.5
1600	ConvMAE-Base	84.6	69.4	52.5	46.5	50.7
	w/ multi-scale decoder	85.0	70.9	53.2	47.1	51.7

Table 6: For a base ConvMAE pretrained for 200 epochs and 1600 epochs, we ablate the multi-scale decoder on ImageNet finetuning and object detection on COCO.

Convolution kernel sizes in stages 1 and 2. Enlarging the kernel size in convolution is shown to be effective for semantic segmentation [44] and visual backbone designs [14, 42]. We also test with enlarging the 5×5 kernel size in stages 1 and 2 to 7×7 and 9×9 . As shown by Table 5, we observe that larger kernel sizes barely influence the performance of ConvMAE on ImageNet-1K accuracy. We hypothesize that the transformer blocks in stage-3 already provide a global FOV which can cancel out the gains introduced from large kernels.

Multi-scale Decoder. In Table 6, we incorporate multi-scale decoder into ConvMAE-base and pretrain for 200 and 1600 epochs. Compared with ConvMAE pretrained 200 epochs, multi-scale decoder can improve classification accuracy, detection AP^{box} , detection AP^{mask} and segmentation mIoU by 0.3%, 0.6% 0.6% and 0.4%, respectively. Given longer pretraining, multi-scale decoder can improve classification accuracy, linear probe accuracy, detection AP^{box} , detection AP^{mask} and segmentation mIoU by 0.4%, 1.6%, 0.7%, 0.6%, 1.0%, respectively. This indicates that fusing multi-grained tokens for mask reconstruction can lead to powerful representations. We will explore more advanced multi-scale decoder architectures such as UNet in the future.

Model Scaling up and down. We design ConvMAE of different parameters scales to match those of MAE-small, MAE-base, MAE-large and MAE-huge. Detailed network architectures are in appendix. The finetuning performances are shown in Table 7. Compared with the original MAE [26] of different scales, our ConvMAE of different scales consistently outperform its MAE counterparts on Imagenet finetuning. This suggests that ConvMAE can be an efficient learner for different paramter scales.

Convergence speed. We compare the convergence of ConvMAE and MAE in terms of ImageNet-1K finetuning, linear probing accuracy and COCO AP^{box} in Figure 3. For fair comparison, ConvMAE and MAE are both pretrained for 1600 epochs. ConvMAE not only attains strong final results but also significantly increases convergence speed on various tasks. Specifically, ConvMAE can surpass the final performance of MAE at 58 epochs on ImageNet-1K finetuning. On COCO object detection, ConvMAE surpasses MAE at 16 epochs, indicating $6.6 \times$ faster convergence speed.

Method	P-Epochs	Model size				
		Small	Base	Base*	Large	Huge
MAE	1600	79.5	83.6	N/A	85.9	86.9
ConvMAE	800	82.6	84.6	84.9	86.2	N/A

Table 7: Ablation study of model scales.

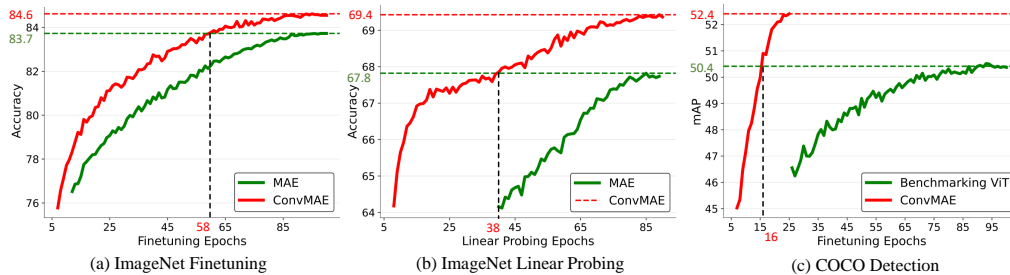


Figure 3: Convergence of MAE and ConvMAE on ImageNet finetuning, ImageNet linear probing, and COCO detection.

5 Conclusion

We propose a simple self-supervised learning framework named as ConvMAE which demonstrate the hybrid local-global blocks [20, 32, 24, 17, 59, 51] can boost the performance of MAE [26] to generate discriminative multi-scale features [36, 56, 41]. The computational efficiency and low pretraining-fineuning gap of original MAE can be well maintained under our ConvMAE. ConvMAE exhibits significantly improved performances on various vision tasks and can be easily implemented. We will study combining improved reconstruction targets with ConvMAE in the future.

References

- [1] Alexei Baevski, Wei-Ning Hsu, Qiantong Xu, Arun Babu, Jiatao Gu, and Michael Auli. Data2vec: A general framework for self-supervised learning in speech, vision and language. *arXiv preprint arXiv:2202.03555*, 2022. 1, 3, 6, 7
- [2] Hangbo Bao, Li Dong, and Furu Wei. Beit: Bert pre-training of image transformers. *arXiv preprint arXiv:2106.08254*, 2021. 1, 2, 3, 5, 6, 8
- [3] Tom Brown, Benjamin Mann, Nick Ryder, Melanie Subbiah, Jared D Kaplan, Prafulla Dhariwal, Arvind Neelakantan, Pranav Shyam, Girish Sastry, Amanda Askell, et al. Language models are few-shot learners. *Advances in neural information processing systems*, 33:1877–1901, 2020. 2
- [4] Nicolas Carion, Francisco Massa, Gabriel Synnaeve, Nicolas Usunier, Alexander Kirillov, and Sergey Zagoruyko. End-to-end object detection with transformers. In *European conference on computer vision*, pages 213–229. Springer, 2020. 2
- [5] Mathilde Caron, Hugo Touvron, Ishan Misra, Hervé Jégou, Julien Mairal, Piotr Bojanowski, and Armand Joulin. Emerging properties in self-supervised vision transformers. In *Proceedings of the IEEE/CVF International Conference on Computer Vision*, pages 9650–9660, 2021. 1, 3, 8
- [6] Ting Chen, Simon Kornblith, Mohammad Norouzi, and Geoffrey Hinton. A simple framework for contrastive learning of visual representations. In *International conference on machine learning*, pages 1597–1607. PMLR, 2020. 3
- [7] Xiaokang Chen, Mingyu Ding, Xiaodi Wang, Ying Xin, Shentong Mo, Yunhao Wang, Shumin Han, Ping Luo, Gang Zeng, and Jingdong Wang. Context autoencoder for self-supervised representation learning. *arXiv preprint arXiv:2202.03026*, 2022. 8
- [8] Xinlei Chen, Saining Xie, and Kaiming He. An empirical study of training self-supervised vision transformers. In *Proceedings of the IEEE/CVF International Conference on Computer Vision*, pages 9640–9649, 2021. 1, 3, 8
- [9] Xiangxiang Chu, Zhi Tian, Bo Zhang, Xinlong Wang, Xiaolin Wei, Huaxia Xia, and Chunhua Shen. Conditional positional encodings for vision transformers. *arXiv preprint arXiv:2102.10882*, 2021. 5
- [10] Zihang Dai, Hanxiao Liu, Quoc Le, and Mingxing Tan. Coatnet: Marrying convolution and attention for all data sizes. *Advances in Neural Information Processing Systems*, 34, 2021. 1, 2, 3, 4
- [11] Navneet Dalal and Bill Triggs. Histograms of oriented gradients for human detection. In *2005 IEEE computer society conference on computer vision and pattern recognition (CVPR’05)*, volume 1, pages 886–893. Ieee, 2005. 7
- [12] Jia Deng, Wei Dong, Richard Socher, Li-Jia Li, Kai Li, and Li Fei-Fei. Imagenet: A large-scale hierarchical image database. In *2009 IEEE conference on computer vision and pattern recognition*, pages 248–255. Ieee, 2009. 1, 6
- [13] Jacob Devlin, Ming-Wei Chang, Kenton Lee, and Kristina Toutanova. Bert: Pre-training of deep bidirectional transformers for language understanding. *arXiv preprint arXiv:1810.04805*, 2018. 1, 2, 3
- [14] Xiaohan Ding, Xiangyu Zhang, Yizhuang Zhou, Jungong Han, Guiguang Ding, and Jian Sun. Scaling up your kernels to 31x31: Revisiting large kernel design in cnns. *arXiv preprint arXiv:2203.06717*, 2022. 9
- [15] Xiaoyi Dong, Jianmin Bao, Ting Zhang, Dongdong Chen, Weiming Zhang, Lu Yuan, Dong Chen, Fang Wen, and Nenghai Yu. Peco: Perceptual codebook for bert pre-training of vision transformers. *arXiv*

- preprint arXiv:2111.12710*, 2021. 3, 8
- [16] Alexey Dosovitskiy, Lucas Beyer, Alexander Kolesnikov, Dirk Weissenborn, Xiaohua Zhai, Thomas Unterthiner, Mostafa Dehghani, Matthias Minderer, Georg Heigold, Sylvain Gelly, et al. An image is worth 16x16 words: Transformers for image recognition at scale. *arXiv preprint arXiv:2010.11929*, 2020. 2
- [17] Stéphane d’Ascoli, Hugo Touvron, Matthew L Leavitt, Ari S Morcos, Giulio Biroli, and Levent Sagun. Convit: Improving vision transformers with soft convolutional inductive biases. In *International Conference on Machine Learning*, pages 2286–2296. PMLR, 2021. 1, 3, 10
- [18] Yuxin Fang, Shusheng Yang, Shijie Wang, Yixiao Ge, Ying Shan, and Xinggang Wang. Unleashing vanilla vision transformer with masked image modeling for object detection. *arXiv preprint arXiv:2204.02964*, 2022. 2, 3, 7
- [19] Peng Gao, Zhengkai Jiang, Haoxuan You, Pan Lu, Steven CH Hoi, Xiaogang Wang, and Hongsheng Li. Dynamic fusion with intra-and inter-modality attention flow for visual question answering. In *Proceedings of the IEEE/CVF conference on computer vision and pattern recognition*, pages 6639–6648, 2019. 2
- [20] Peng Gao, Jiasen Lu, Hongsheng Li, Roozbeh Mottaghi, and Aniruddha Kembhavi. Container: Context aggregation network. *arXiv preprint arXiv:2106.01401*, 2021. 1, 2, 3, 4, 5, 10
- [21] Peng Gao, Minghang Zheng, Xiaogang Wang, Jifeng Dai, and Hongsheng Li. Fast convergence of detr with spatially modulated co-attention. In *Proceedings of the IEEE/CVF International Conference on Computer Vision*, pages 3621–3630, 2021. 3
- [22] Benjamin Graham, Martin Engelcke, and Laurens Van Der Maaten. 3d semantic segmentation with submanifold sparse convolutional networks. In *Proceedings of the IEEE conference on computer vision and pattern recognition*, pages 9224–9232, 2018. 2
- [23] Benjamin Graham and Laurens van der Maaten. Submanifold sparse convolutional networks. *arXiv preprint arXiv:1706.01307*, 2017. 2, 5
- [24] Jianyuan Guo, Kai Han, Han Wu, Chang Xu, Yehui Tang, Chunjing Xu, and Yunhe Wang. Cmt: Convolutional neural networks meet vision transformers. *arXiv preprint arXiv:2107.06263*, 2021. 3, 5, 10
- [25] Kai Han, An Xiao, Enhua Wu, Jianyuan Guo, Chunjing Xu, and Yunhe Wang. Transformer in transformer. *Advances in Neural Information Processing Systems*, 34, 2021. 3
- [26] Kaiming He, Xinlei Chen, Saining Xie, Yanghao Li, Piotr Dollár, and Ross Girshick. Masked autoencoders are scalable vision learners. *arXiv preprint arXiv:2111.06377*, 2021. 1, 2, 3, 4, 5, 6, 8, 9, 10
- [27] Kaiming He, Haoqi Fan, Yuxin Wu, Saining Xie, and Ross Girshick. Momentum contrast for unsupervised visual representation learning. In *Proceedings of the IEEE/CVF conference on computer vision and pattern recognition*, pages 9729–9738, 2020. 3, 7, 8
- [28] Kaiming He, Georgia Gkioxari, Piotr Dollár, and Ross Girshick. Mask r-cnn. In *Proceedings of the IEEE international conference on computer vision*, pages 2961–2969, 2017. 1, 2, 3, 6, 7
- [29] Kaiming He, Xiangyu Zhang, Shaoqing Ren, and Jian Sun. Deep residual learning for image recognition. In *Proceedings of the IEEE conference on computer vision and pattern recognition*, pages 770–778, 2016. 2
- [30] Ajay Jain, Pieter Abbeel, and Deepak Pathak. Locally masked convolution for autoregressive models. In *Conference on Uncertainty in Artificial Intelligence*, pages 1358–1367. PMLR, 2020. 2
- [31] Alex Krizhevsky, Ilya Sutskever, and Geoffrey E Hinton. Imagenet classification with deep convolutional neural networks. *Advances in neural information processing systems*, 25, 2012. 1, 2
- [32] Kunchang Li, Yali Wang, Junhao Zhang, Peng Gao, Guanglu Song, Yu Liu, Hongsheng Li, and Yu Qiao. Uniformer: Unifying convolution and self-attention for visual recognition. *arXiv preprint arXiv:2201.09450*, 2022. 1, 2, 3, 4, 5, 10
- [33] Yanghao Li, Hanzi Mao, Ross Girshick, and Kaiming He. Exploring plain vision transformer backbones for object detection. *arXiv preprint arXiv:2203.16527*, 2022. 3, 7
- [34] Yanghao Li, Chao-Yuan Wu, Haoqi Fan, Karttikeya Mangalam, Bo Xiong, Jitendra Malik, and Christoph Feichtenhofer. Improved multiscale vision transformers for classification and detection. *arXiv preprint arXiv:2112.01526*, 2021. 2, 7
- [35] Yanghao Li, Saining Xie, Xinlei Chen, Piotr Dollár, Kaiming He, and Ross Girshick. Benchmarking detection transfer learning with vision transformers. *arXiv preprint arXiv:2111.11429*, 2021. 3, 5, 7
- [36] Tsung-Yi Lin, Piotr Dollár, Ross Girshick, Kaiming He, Bharath Hariharan, and Serge Belongie. Feature pyramid networks for object detection. In *Proceedings of the IEEE conference on computer vision and pattern recognition*, pages 2117–2125, 2017. 3, 6, 10
- [37] Tsung-Yi Lin, Priya Goyal, Ross Girshick, Kaiming He, and Piotr Dollár. Focal loss for dense object detection. In *Proceedings of the IEEE international conference on computer vision*, pages 2980–2988, 2017. 2
- [38] Tsung-Yi Lin, Michael Maire, Serge Belongie, James Hays, Pietro Perona, Deva Ramanan, Piotr Dollár, and C Lawrence Zitnick. Microsoft coco: Common objects in context. In *European conference on computer vision*, pages 740–755. Springer, 2014. 7
- [39] Guilin Liu, Fitsum A Reda, Kevin J Shih, Ting-Chun Wang, Andrew Tao, and Bryan Catanzaro. Image inpainting for irregular holes using partial convolutions. In *Proceedings of the European conference on computer vision (ECCV)*, pages 85–100, 2018. 2
- [40] Shilong Liu, Feng Li, Hao Zhang, Xiao Yang, Xianbiao Qi, Hang Su, Jun Zhu, and Lei Zhang. Dab-detr: Dynamic anchor boxes are better queries for detr. *arXiv preprint arXiv:2201.12329*, 2022. 3

- [41] Ze Liu, Yutong Lin, Yue Cao, Han Hu, Yixuan Wei, Zheng Zhang, Stephen Lin, and Baining Guo. Swin transformer: Hierarchical vision transformer using shifted windows. In *Proceedings of the IEEE/CVF International Conference on Computer Vision*, pages 10012–10022, 2021. [1](#), [2](#), [3](#), [5](#), [7](#), [8](#), [10](#)
- [42] Zhuang Liu, Hanzi Mao, Chao-Yuan Wu, Christoph Feichtenhofer, Trevor Darrell, and Saining Xie. A convnet for the 2020s. *arXiv preprint arXiv:2201.03545*, 2022. [9](#)
- [43] Ilya Loshchilov and Frank Hutter. Decoupled weight decay regularization. In *International Conference on Learning Representations*, 2018. [7](#)
- [44] Chao Peng, Xiangyu Zhang, Gang Yu, Guiming Luo, and Jian Sun. Large kernel matters—improve semantic segmentation by global convolutional network. In *Proceedings of the IEEE conference on computer vision and pattern recognition*, pages 4353–4361, 2017. [9](#)
- [45] Alec Radford, Jong Wook Kim, Chris Hallacy, Aditya Ramesh, Gabriel Goh, Sandhini Agarwal, Girish Sastry, Amanda Askell, Pamela Mishkin, Jack Clark, et al. Learning transferable visual models from natural language supervision. In *International Conference on Machine Learning*, pages 8748–8763. PMLR, 2021. [2](#)
- [46] Alec Radford, Jeffrey Wu, Rewon Child, David Luan, Dario Amodei, Ilya Sutskever, et al. Language models are unsupervised multitask learners. *OpenAI blog*, 1(8):9, 2019. [2](#)
- [47] Aditya Ramesh, Mikhail Pavlov, Gabriel Goh, Scott Gray, Chelsea Voss, Alec Radford, Mark Chen, and Ilya Sutskever. Zero-shot text-to-image generation. In *International Conference on Machine Learning*, pages 8821–8831. PMLR, 2021. [8](#)
- [48] Joseph Redmon, Santosh Divvala, Ross Girshick, and Ali Farhadi. You only look once: Unified, real-time object detection. In *Proceedings of the IEEE conference on computer vision and pattern recognition*, pages 779–788, 2016. [2](#)
- [49] Mengye Ren, Andrei Pokrovsky, Bin Yang, and Raquel Urtasun. Sbnnet: Sparse blocks network for fast inference. In *Proceedings of the IEEE Conference on Computer Vision and Pattern Recognition*, pages 8711–8720, 2018. [2](#), [5](#)
- [50] Shaoqing Ren, Kaiming He, Ross Girshick, and Jian Sun. Faster r-cnn: Towards real-time object detection with region proposal networks. *Advances in neural information processing systems*, 28, 2015. [2](#)
- [51] Aravind Srinivas, Tsung-Yi Lin, Niki Parmar, Jonathon Shlens, Pieter Abbeel, and Ashish Vaswani. Bottleneck transformers for visual recognition. In *Proceedings of the IEEE/CVF conference on computer vision and pattern recognition*, pages 16519–16529, 2021. [1](#), [3](#), [4](#), [10](#)
- [52] Hao Tan and Mohit Bansal. Lxmert: Learning cross-modality encoder representations from transformers. *arXiv preprint arXiv:1908.07490*, 2019. [2](#)
- [53] Hugo Touvron, Matthieu Cord, Matthijs Douze, Francisco Massa, Alexandre Sablayrolles, and Hervé Jégou. Training data-efficient image transformers & distillation through attention. In *International Conference on Machine Learning*, pages 10347–10357. PMLR, 2021. [3](#), [8](#)
- [54] Hugo Touvron, Matthieu Cord, Alaaeldin El-Nouby, Jakob Verbeek, and Hervé Jégou. Three things everyone should know about vision transformers. *arXiv preprint arXiv:2203.09795*, 2022. [2](#), [3](#)
- [55] Ashish Vaswani, Noam Shazeer, Niki Parmar, Jakob Uszkoreit, Llion Jones, Aidan N Gomez, Łukasz Kaiser, and Illia Polosukhin. Attention is all you need. *Advances in neural information processing systems*, 30, 2017. [2](#)
- [56] Wenhai Wang, Enze Xie, Xiang Li, Deng-Ping Fan, Kaitao Song, Ding Liang, Tong Lu, Ping Luo, and Ling Shao. Pyramid vision transformer: A versatile backbone for dense prediction without convolutions. In *Proceedings of the IEEE/CVF International Conference on Computer Vision*, pages 568–578, 2021. [1](#), [3](#), [10](#)
- [57] Chen Wei, Haoqi Fan, Saining Xie, Chao-Yuan Wu, Alan Yuille, and Christoph Feichtenhofer. Masked feature prediction for self-supervised visual pre-training. *arXiv preprint arXiv:2112.09133*, 2021. [1](#), [3](#), [6](#), [7](#)
- [58] Haiping Wu, Bin Xiao, Noel Codella, Mengchen Liu, Xiyang Dai, Lu Yuan, and Lei Zhang. Cvt: Introducing convolutions to vision transformers. In *Proceedings of the IEEE/CVF International Conference on Computer Vision*, pages 22–31, 2021. [3](#)
- [59] Tete Xiao, Piotr Dollar, Mannat Singh, Eric Mintun, Trevor Darrell, and Ross Girshick. Early convolutions help transformers see better. *Advances in Neural Information Processing Systems*, 34, 2021. [1](#), [2](#), [3](#), [4](#), [10](#)
- [60] Tete Xiao, Yingcheng Liu, Bolei Zhou, Yuning Jiang, and Jian Sun. Unified perceptual parsing for scene understanding. In *Proceedings of the European Conference on Computer Vision (ECCV)*, pages 418–434, 2018. [1](#), [2](#), [3](#), [6](#), [7](#)
- [61] Zhenda Xie, Zheng Zhang, Yue Cao, Yutong Lin, Jianmin Bao, Zhuliang Yao, Qi Dai, and Han Hu. Simmim: A simple framework for masked image modeling. *arXiv preprint arXiv:2111.09886*, 2021. [2](#), [6](#), [7](#)
- [62] Zhenda Xie, Zheng Zhang, Xizhou Zhu, Gao Huang, and Stephen Lin. Spatially adaptive inference with stochastic feature sampling and interpolation. In *European conference on computer vision*, pages 531–548. Springer, 2020. [2](#)
- [63] Li Yuan, Yunpeng Chen, Tao Wang, Weihao Yu, Yujun Shi, Zi-Hang Jiang, Francis EH Tay, Jiashi Feng, and Shuicheng Yan. Tokens-to-token vit: Training vision transformers from scratch on imagenet. In *Proceedings of the IEEE/CVF International Conference on Computer Vision*, pages 558–567, 2021. [3](#)
- [64] Gongjie Zhang, Zhipeng Luo, Yingchen Yu, Kaiwen Cui, and Shijian Lu. Accelerating detr convergence via semantic-aligned matching. *arXiv preprint arXiv:2203.06883*, 2022. [3](#)
- [65] Bolei Zhou, Hang Zhao, Xavier Puig, Tete Xiao, Sanja Fidler, Adela Barriuso, and Antonio Torralba. Semantic understanding of scenes through the ade20k dataset. *International Journal of Computer Vision*,

Model	$[C_1, C_2, C_3]$	$[L_1, L_2, L_3]$	$[E_1, E_2, E_3]$	$[P_1, P_2, P_3]$	H_a	#Params (M)
ConvMAE-S	[128, 256, 384]	[2, 2, 11]	[56, 28, 14]	[4, 4, 4]	6	22
ConvMAE-B	[256, 384, 768]	[2, 2, 11]	[56, 28, 14]	[4, 4, 4]	12	84
ConvMAE-B*	[256, 384, 768]	[2, 2, 11]	[56, 28, 14]	[8, 8, 4]	12	88
ConvMAE-L	[384, 768, 1024]	[2, 2, 23]	[56, 28, 14]	[8, 8, 4]	16	322
ConvMAE-H	[768, 1024, 1280]	[2, 2, 31]	[56, 28, 14]	[8, 8, 4]	16	666

Table 8: Architecture details of ConvMAE small, base, large and huge. ConvMAE-B* represents multi-scale encoder with large mlp-ratios in stage 1 and stage 2. $[C_1, C_2, C_3]$, $[L_1, L_2, L_3]$, $[E_1, E_2, E_3]$ and $[P_1, P_2, P_3]$ represents channel dimension, number of layer, spatial resolution and mlp-ratios for each stage 1, stage 2 and stage 3. H_a stands for the number of attention heads in stage 3.

127(3):302–321, 2019. 7

- [66] Jinghao Zhou, Chen Wei, Huiyu Wang, Wei Shen, Cihang Xie, Alan Yuille, and Tao Kong. ibot: Image bert pre-training with online tokenizer. *arXiv preprint arXiv:2111.07832*, 2021. 1, 3
- [67] Xizhou Zhu, Weijie Su, Lewei Lu, Bin Li, Xiaogang Wang, and Jifeng Dai. Deformable detr: Deformable transformers for end-to-end object detection. *arXiv preprint arXiv:2010.04159*, 2020. 3

6 Appendix

Architecture Details of ConvMAE Encoder. The details of our hybrid convolution-transformer encoder is explained below. Given an input image $I \in \mathbb{R}^{3 \times H \times W}$, stage 1 of ConvMAE encoder generates a high-resolution token embeddings $E_1 \in \mathbb{R}^{C_1 \times \frac{H}{4} \times \frac{W}{4}}$ using non-overlapping 4×4 strided convolution firstly. Then E_1 is feed into stacked convolutional blocks which is repeated L_1 times, where L_1 stands for the number of layers in stage 1. Similar as stage 1, stage 2 further downsamples feature map into token embeddings $E_2 \in \mathbb{R}^{C_2 \times \frac{H}{8} \times \frac{W}{8}}$ using non-overlapping 2×2 strided convolution. E_2 is processed by L_2 layers of convolutional blocks again. After local information fusion utilized in stage 1 and stage 2, stage 3 perform global feature fusion using transformer block. E_2 is projected into tokens embeddings $E_3 \in \mathbb{R}^{(\frac{H}{16} \times \frac{W}{16}) \times C_3}$ using non-overlapping 2×2 strided convolution. E_3 mixing with Intermediate Positional Embedding (IPL) is feed into a pure transformer block with L_3 layers. We denote the number of attention heads in stage 3 as H_a . The mlp-ratios in FFN for different stages is denoted as P_1, P_2 and P_3 in respectively. Stage 1 and stage 2 is designed to capture fine-grained details on high resolution feature map. Stage 3 can perform dynamically global reasoning efficiently on a rather low-resolution feature map. At the same time, stage 3 can enlarge the filed-of-view (FOV) of backbone which benefits a wide range of downstream tasks. The encoder of ConvMAE can seamlessly inherits the merits of convolution and transformer block. The architecture details for small, base and large model is listed in Table 8. ConvMAE small, base, large and huge share similar parameter scale with the encoder of MAE-small, MAE-base, MAE-large and MAE-huge.